

# Controlled Synthesis and Catalytic Properties of Supported In-Pd Intermetallic Compounds

*Matthias Neumann<sup>1</sup>, Detre Teschner<sup>2</sup>, Axel Knop-Gericke<sup>2</sup>, Wladimir Reschetilowski<sup>3</sup>, Marc  
Armbüster<sup>\*4</sup>*

<sup>1</sup> Max-Planck Institut für Chemische Physik fester Stoffe, Nöthnitzer Str. 40, 01187 Dresden,  
Germany

<sup>2</sup> Fritz-Haber-Institut der Max-Planck-Gesellschaft, Faradayweg 4-6, 14195 Berlin, Germany

<sup>3</sup> Chair for Industrial Chemistry, TU Dresden, 01062 Dresden, Germany

<sup>4</sup> Faculty of Natural Sciences, Institute of Chemistry, Materials for Innovative Energy Concepts,  
Technische Universität Chemnitz, 09107 Chemnitz, Germany

## HIGHLIGHTS

Controlled synthesis of supported intermetallic In-Pd compounds.

High selectivity of In-Pd compounds in the steam reforming of methanol.

Long-term measurements ~~pröove~~prove the stability of In-Pd/In<sub>2</sub>O<sub>3</sub> in MSR.

## KEYWORDS

17 InPd, In<sub>3</sub>Pd<sub>2</sub>, In<sub>7</sub>Pd<sub>3</sub>, In<sub>2</sub>O<sub>3</sub>, MSR, CO<sub>2</sub> selective, methanol steam reforming

## 18 ABSTRACT

19 DTA/TG/MS measurements were used to investigate the temperature-dependent and successive  
20 phase formation of different intermetallic In-Pd compounds by controlled reduction of  
21 PdO/In<sub>2</sub>O<sub>3</sub> with hydrogen. Reduction procedures were developed to obtain supported  
22 intermetallic InPd and In<sub>3</sub>Pd<sub>2</sub> particles by reactive metal-support interaction (RMSI) without  
23 detectable amounts of other compounds. In<sub>7</sub>Pd<sub>3</sub> could only be obtained in admixture with  
24 elemental indium due to the direct reduction of the In<sub>2</sub>O<sub>3</sub> support at temperatures above 350 °C.

25 All materials exhibit catalytic activity for methanol steam reforming and exhibit high CO<sub>2</sub>  
26 selectivities up to 98%. Long-term measurements proved the superior stability of the In-Pd/In<sub>2</sub>O<sub>3</sub>  
27 materials in comparison to Cu-based systems over 100 hours time on stream with high  
28 selectivity.

29

## 30 1 Introduction

31 The depletion of fossil energy carriers as well as the increasing demand of energy worldwide led  
32 to an intensification in the research for alternative energy sources. Renewable energies and  
33 secondary energy carriers like hydrogen have gained much attention in the recent years  
34 especially with the advances of fuel cell technology.<sup>1-5</sup>

35 Hydrogen is today mainly produced by reforming of hydrocarbons.<sup>6-8</sup> Another possibility  
36 intensively studied momentarily is the development of better electrodes for electrochemical

water splitting.<sup>9-10</sup> Hydrogen itself has a relatively low volumetric energy density (0.0107 MJ/L<sup>11</sup>). Therefore it has to be compressed or liquefied to improve the transportation efficiency. Besides the physical storage of hydrogen the chemical storage in form of metal hydrides or small chemical compounds, e.g. methanol, is likely to be of great importance and is studied broadly.<sup>12</sup> Up to now, the storage capacity in metal hydrides is too low and lacks materials exhibiting easy and fast hydrogen charging and discharging.<sup>3-4</sup> Compared to gasoline (34.2 MJ/L<sup>11</sup>), methanol has a relatively high energy density per volume (16 MJ/L<sup>13</sup>) and is a liquid, easing handling and transport. The often discussed drawback of the toxicity of methanol relativizes comparing the LD50<sub>oral</sub> values of methanol (rat ~ 5600 mg/kg<sup>14</sup>) and gasoline (rat ~ 15000 mg/kg<sup>15</sup>) and considering the carcinogenic effects of the latter. This makes methanol a promising hydrogen storage candidate with high potential in a future hydrogen-based energy infrastructure.

Methanol steam reforming (MSR) is a smart method to release the chemically stored hydrogen from methanol and water mixtures.<sup>16</sup> Thereby methanol is reacting with one water molecule forming three molecules of hydrogen and the byproduct CO<sub>2</sub> according to reaction equation 1.



Besides this preferred reaction, decomposition of methanol can take place (equation 2) leading to a lower hydrogen content in the product stream and, more important, to the formation of CO. To ensure most efficient use of hydrogen in PEM fuel cells, the CO concentration has to be lower than 10-30 ppm since higher contents lead to strong deactivation of the PEM fuel cell.<sup>17</sup> Therefore a high selectivity towards steam reforming instead of methanol decomposition has to

be ensured. To complicate things, both reaction pathways are linked by the water gas shift reaction (equation 3).



Cu/ZnO/Al<sub>2</sub>O<sub>3</sub> catalysts can be applied to methanol steam reforming, showing high activity and selectivity.<sup>16</sup> The major drawback of these catalysts is a high deactivation rate, especially at temperatures above 300 °C due to sintering of the copper particles.<sup>18</sup> Materials circumventing deactivation were found by Iwasa *et al.* who investigated several noble metal-based catalytic systems with easily reducible oxides as support.<sup>19-21</sup> After reduction at elevated temperatures intermetallic compounds like ZnPd (from Pd/ZnO) or InPd (from Pd/In<sub>2</sub>O<sub>3</sub>) are formed by reactive metal-support interaction (RMSI<sup>22</sup>) reaction of palladium with the reduced metal atoms from the oxide. Since then several studies have been published on In-Pd-based catalysts and their physical and catalytic properties.<sup>23-27</sup> The presence of intermetallic compounds improved the CO<sub>2</sub>-selectivity of the catalysts to above 95%. These materials are also much more resistant against sintering, showing higher stability at temperatures above 300 °C compared to Cu-based systems.<sup>18, 28-29</sup> Up to now most effort has been put into investigating the roles of the different phases in ZnPd/ZnO catalysts,<sup>30-33</sup> revealing an interplay between ZnO and ZnPd being responsible for the observed excellent selectivity – and not the sheer presence of the intermetallic compound ZnPd.<sup>34</sup> At 300 °C pre-reduced Pd/In<sub>2</sub>O<sub>3</sub> samples showed up to 95.5% selectivity for MSR.<sup>20, 35</sup> Men *et al.* prepared In-Pd/Al<sub>2</sub>O<sub>3</sub> samples with various In-Pd ratios. They found that the CO<sub>2</sub>-selectivity is increasing with higher In/Pd ratios. After catalytic testing up to 450 °C the supported samples contained InPd.<sup>25</sup> Lorenz *et al.* obtained different In-Pd intermetallic compounds during stepwise reduction of Pd/In<sub>2</sub>O<sub>3</sub> exhibiting high selectivities for MSR. At reaction temperatures above 400 °C the intermetallic compounds were encapsulated with an

In<sub>2</sub>O<sub>3</sub> shell reducing the accessible surface.<sup>23</sup> Rameshan *et al.* investigated near-surface intermetallic In-Pd phases (NSIPs<sup>36</sup>) in MSR by near-ambient pressure XPS (NAP-XPS) measurements. They supposed the interplay between the oxide and the intermetallic compound also to play a crucial rule on the selectivity in methanol steam reforming on In-Pd materials.<sup>36</sup> Although there are several publications on In-Pd/In<sub>2</sub>O<sub>3</sub> materials, there is no detailed investigation available dealing with the successive formation of In-Pd intermetallic compounds. Therefore the aim of this work is to close this gap by investigating the processes occurring during reduction of PdO/In<sub>2</sub>O<sub>3</sub> by *in situ* DTA/TG/MS measurements, NAP-XPS as well as powder X-ray diffraction (XRD) to identify crystalline phases. In addition, this study gives detailed insight into the catalytic activity and selectivity in the steam reforming of methanol of the respective intermetallic compounds supported on In<sub>2</sub>O<sub>3</sub>.

## 2 Experimental

### 2.1 Catalyst preparation

10 wt% Pd/In<sub>2</sub>O<sub>3</sub> was prepared by wet impregnation using Pd(NO<sub>3</sub>)<sub>2</sub>·2 H<sub>2</sub>O (Sigma Aldrich, ~40% Pd) on In<sub>2</sub>O<sub>3</sub> (Chempur, >99.99%) according to procedures described in the literature.<sup>23</sup> For a typical impregnation 3.5 g In<sub>2</sub>O<sub>3</sub> were suspended in a solution of 1.042 g Pd(NO<sub>3</sub>)<sub>2</sub>·2 H<sub>2</sub>O in 20 mL deionized water with 2-3 drops of concentrated nitric acid (Sigma-Aldrich, >65%). Subsequently, 200 mL of deionized water were added and the resulting mixture was stirred for 30 minutes prior to the removal of the water in vacuum at 70 °C. The impregnated sample was calcined at 400 °C for three hours in synthetic air (Air Liquide, 20.5% O<sub>2</sub> in N<sub>2</sub>). A 10 wt% Pd/SiO<sub>2</sub> sample (SiO<sub>2</sub>: Wacker, HDK-N20) was prepared using the same procedure.

For comparison a conventional Cu/ZnO/Al<sub>2</sub>O<sub>3</sub> catalyst with a molar composition of the metal oxides of 67.5/22.5/10 was prepared by co-precipitation from the respective nitrates according to literature.<sup>37</sup> 20.667 g Cu(NO<sub>3</sub>)<sub>2</sub>·3 H<sub>2</sub>O (Merck, 99.5%), 23.522 g Zn(NO<sub>3</sub>)<sub>2</sub>·4 H<sub>2</sub>O (Merck, 98.5%) and 26.079 g Al(NO<sub>3</sub>)<sub>3</sub>·9 H<sub>2</sub>O (Grüssing, 98%) were dissolved in 500 mL of a 1:1 ethanol-water mixture (v/v) (ethanol: Roth, 99.8%) and quickly added to a solution of 52.99 g Na<sub>2</sub>CO<sub>3</sub> (Grüssing, 99.5%) in 500 mL 1:1 ethanol-water mixture (v/v). The resulting gel was aged for 1.5 h at 40 °C. Subsequently the precipitate was filtered and washed several times with deionized water. The product was dried at 90 °C for five hours prior to calcination in synthetic air with a heating-rate of 3 K/min and holding for 12 hours at 400 °C.

## 2.2 Characterization

Chemical composition of the materials were obtained by ICP-OES (*Vista RL*, Varian). All samples were dissolved in aqua regia and measured in triplicate. Oxygen content of the samples was determined by carrier gas hot extraction (*TCH 600*, Leco). DTA/TG/MS measurements were conducted in a Netzsch *STA 448 F3 Jupiter*® combined with a Pfeiffer *Omnistar* quadrupole mass spectrometer on approximately 80 mg samples. The high resolution of 1 µg makes the TG measurements a valuable method for the investigation of small mass changes in reactive atmosphere and the rather high amount of sample results in a standard deviation of less than 0.01 wt%. For the DTA/TG/MS measurements the samples were heated with 5 K/min to 200 °C and cooled down to room temperature again to desorb moisture and other volatile compounds prior to the reductive treatment. Gas flows during the measurements (10 vol% hydrogen in helium for reduction) with a total flow of 50 mL/min were provided by mass flow controllers (Bronkhorst).

All DTA/TG/MS measurements are corrected by blank measurements to account for any non-sample effects. Low temperature-programmed reduction (TPR) was measured in the range of -80 °C up to 550 °C with a Thermo *TPDRO 1100* in 10 vol% hydrogen in argon (total flow 20 mL/min). Prior to reduction, samples were pretreated in 5 vol% oxygen in helium (total flow 20 mL/min) heating with 5 K/min and holding 1 hour at 400 °C. All samples were characterized by powder X-ray diffraction (XRD) with a *Huber G670* (Guinier geometry, Cu K $\alpha_1$  radiation  $\lambda$  = 1.54060 Å, quartz monochromator, image plate detector) to identify crystalline phases during reduction and catalytic measurements. XRD patterns were fitted using the program PowderCell to estimate the content of the phases and their crystallite size.<sup>38</sup>

### 2.3 Near-ambient pressure XPS measurements

NAP-XPS measurements of supported PdO/In<sub>2</sub>O<sub>3</sub> were recorded at the ISIS-PGM beamline at BESSY II (Helmholtz Zentrum Berlin für Materialien und Energie GmbH) to give detailed insight into the formation of intermetallic In-Pd species during reduction and under MSR conditions. The experimental setup is described in literature.<sup>39</sup> For the NAP-XPS measurements, samples were prepared as thin discs (with a diameter of 8 mm) using 1 g PdO/In<sub>2</sub>O<sub>3</sub> pressed with 1.5 tons in air. Samples were first measured as prepared under UHV conditions before being reduced in 0.5 mbar H<sub>2</sub> up to 390 °C. Methanol steam reforming conditions were subsequently applied (total pressure of 0.2 mbar, water-to-methanol ratio 2:1) while heating the samples up to 360 °C. In3d, In4d, Pd3d, Pd3p, O1s and C1s spectra were recorded with three different information depths by varying the photon energy of the incoming beam. The resulting kinetic energies of 232, 532 and 832 eV reveal in information depths of approximately 1.9, 3.2 and 4.4 nm, respectively.<sup>40</sup> All spectra were energy corrected using the carbon C1s signal at 284.8 eV.<sup>41</sup> The XP spectra were processed in the software *CasaXPS* and a Shirley background was

subtracted.<sup>42-43</sup> Because of the strong overlap of the intermetallic and oxidic indium signals it was not possible to deconvolute the different indium species from the In3d or the In4d signal. The ratio of  $\text{In}_{\text{total}}/\text{Pd}_{\text{total}}$  was calculated considering the peak areas of the respective 3d signals, the photon flux, the ring current and the cross section of the respective elemental species.<sup>44</sup> To obtain the oxygen content the O1s signal at 532 eV was used. The Pd3p<sub>3/2</sub> contribution in the energy range of the O1s signal was determined from the Pd3p<sub>1/2</sub> signal applying a fixed area ratio of 1:2 and a spin-orbit coupling of 27.8 eV. The corrected oxygen O1s signal was fitted by a symmetric Gaussian/Lorentzian (70:30) peak.

## 2.4 Catalytic testing

Catalytic tests were conducted in a fixed-bed flow reactor between 260 °C and 350 °C. For comparison a Cu/ZnO/Al<sub>2</sub>O<sub>3</sub> and a 10 wt% Pd/SiO<sub>2</sub> catalyst were tested under identical conditions. The respective In-Pd intermetallic compounds were formed by *in situ* pre-reduction of the PdO/In<sub>2</sub>O<sub>3</sub> inside the fixed-bed flow reactor directly before the catalytic measurements. The homogeneous reactant flow of premixed methanol and water with a molar ratio of 1:1 was provided by a Bronkhorst  $\mu$ -Flow mass flow controller connected to an evaporator. To separate the unconverted reactants from the product stream a Nafion<sup>®</sup> membrane (Perma Pure) was used. During all catalytic measurements the membrane was flushed with 10 L/h nitrogen in counter flow mode to dry the product stream. A HP-GC 5890 series II equipped with a TCD and a GS-Gaspro column (30 m \* 0.32  $\mu$ m) was used to analyze the formed hydrogen in the product stream. An FT-IR multigas detector DX2000 (Gasmeter) measured the CO and CO<sub>2</sub> concentration simultaneously down into the low ppm range. The rate of methanol conversion is calculated

according to equation (4), while the CO<sub>2</sub>-selectivity is calculated according to equation (5), which is justified by the fact that no by-products besides CO were detected. For comparison of the selectivities the space time velocity was adjusted to achieve 30% methanol conversion for all materials. Apparent activation energies were derived from Arrhenius plots. XRD measurements of the samples after the catalytic test in MSR were performed *ex situ* in air.

$$k = \frac{\text{mmol MeOH}}{\text{mmol transition metal} \times s} \quad \text{eq. (4)}$$

$$S_{CO_2, X=30\%} = \frac{c_{CO_2}}{c_{CO_2} + c_{CO}} \quad \text{eq. (5)}$$

### 3 Results and discussion

The idea of this work is to obtain different supported intermetallic compounds by controlled reduction starting from the same material for a better comparison of the intrinsic properties. Therefore, the first step was to synthesize an impregnated 10 wt% Pd on In<sub>2</sub>O<sub>3</sub> sample. This sample was the starting point for all following experiments. Through subsequent and stepwise reduction it should be possible to obtain different intermetallic In-Pd compounds by reactive metal-support interaction (RMSI [50]) starting from elemental palladium which is activating the hydrogen to facilitate the reduction of the In<sub>2</sub>O<sub>3</sub> support. The resulting elemental indium is diffusing into the palladium which should first result in the formation of a palladium-rich alloy according to the binary In-Pd phase diagram.<sup>45</sup> With ongoing reduction of the In<sub>2</sub>O<sub>3</sub>, more indium-rich intermetallic compounds like InPd<sub>2</sub>, In<sub>2</sub>Pd<sub>3</sub> and InPd should form. Loosing it's elemental character, the palladium in the formed intermetallic compounds is less prone to activate the hydrogen needed for further reduction of the In<sub>2</sub>O<sub>3</sub> support, e.g. due to the absence

of hydride formation.<sup>46</sup> To overcome this decreasing reduction potential, the temperature has to be increased for further reduction of the support. The aim of this work was to establish different reduction procedures which are suitable to lead to the formation of only one specific intermetallic In-Pd compound without other metallic phases being present.

### 3.1 Synthesis, Characterization and Reduction of PdO/In<sub>2</sub>O<sub>3</sub>

According to elemental analysis by ICP-OES, the calcined PdO/In<sub>2</sub>O<sub>3</sub> sample contains 9.44(6) wt% palladium, corresponding to a 9.57(6) wt% Pd/In<sub>2</sub>O<sub>3</sub> material. XRD analysis of the as-prepared sample only shows reflections of In<sub>2</sub>O<sub>3</sub>, meaning that the size of the PdO crystallites is below the necessary coherence length for the diffraction experiment.

To investigate if the reduction steps are well resolved from each other, a first DTA/TG/MS measurement up to 600 °C of PdO/In<sub>2</sub>O<sub>3</sub> in 10% H<sub>2</sub>/He was conducted. The measurement revealed several reduction steps as shown in Figure 1. From the point of the steepest slope of the TG trace the optimum temperature for the highest formation rate of the respective compound could be determined. At these temperatures also the m/z signal of 18 – assigned to water – is showing its maxima. The corresponding DTA signals are too weak and could not be taken for further explanations due to overlapping processes. The overall mass loss after the reductive treatment of 16.5(1) wt% correlates well to the total oxygen content of the sample (16.6(2) wt% determined by chemical analysis, expected 16.8 wt% for PdO and In<sub>2</sub>O<sub>3</sub>) implying that under these harsh conditions the material – including the support – is fully reduced. From the slope of the TG signal three optimized reduction procedures were developed accordingly to interrupt the phase formation obtaining only the target intermetallic compound in a supported state. The

optimized procedures were subsequently applied during DTA/TG/MS (Figure 2) and TPR measurements (Figure 3). Phases formed during the reductive treatments were identified by XRD after the experiments (Figure 4). The results of the DTA/TG/MS measurements are summarized in Table 1.

Table 1: Summary of the expected and observed mass losses

reduction procedure	reaction	expected mass loss / wt%	observed mass loss / wt%
25 °C (RT)	$34 \text{ PdO} + 43 \text{ H}_2 + 3 \text{ In}_2\text{O}_3 \rightarrow \text{"In15Pd85"} + 43 \text{ H}_2\text{O}$	1.8	1.8(1)
300 °C, 1h	$20 \text{ "In15Pd85"} + 21 \text{ H}_2 + 7 \text{ In}_2\text{O}_3 \rightarrow 17 \text{ InPd} + 21 \text{ H}_2\text{O}$	1.7	1.7(1)
390 °C, 1h	$4 \text{ InPd} + 3 \text{ H}_2 + \text{In}_2\text{O}_3 \rightarrow 2 \text{ In}_3\text{Pd}_2 + 3 \text{ H}_2\text{O}$	1.1	1.0(1)
550 °C, 3h	$6 \text{ In}_3\text{Pd}_2 + 15 \text{ H}_2 + 5 \text{ In}_2\text{O}_3 \rightarrow 4 \text{ In}_7\text{Pd}_3 + 15 \text{ H}_2\text{O}$ $\text{In}_2\text{O}_3 + 3 \text{ H}_2 \rightarrow 2 \text{ In} + 3 \text{ H}_2\text{O}$	1.8 10.1 (max)	11.4(1)
sum	-	16.5	15.9(1)
600 °C, 5h	-		16.5(1)

DTA revealed that the first reduction step occurring directly after switching to reducing atmosphere is highly exothermic (Figure 1). The low-temperature TPR measurement also showed significant hydrogen consumption around ambient temperature. In agreement with the mass loss of 1.8(1) wt% at 25 °C, this step is assigned to the reduction of PdO to palladium. For this reaction a mass loss of only 1.4 wt% is calculated and the difference can be explained by a simultaneous reduction of In<sub>2</sub>O<sub>3</sub> by highly reducing palladium hydride leading directly to the formation of a palladium rich alloy (In15Pd85). The observed mass loss is significantly lower than one would expect for the formation of any intermetallic In-Pd compound. The TPR

measurements exhibit a negative signal indicating hydrogen release directly after the first reduction step between 50 °C and 150 °C. It is known from literature that palladium is prone to hydride formation at ambient temperature.<sup>47-48</sup> The decomposition of the hydride is observed in the TPR measurement, however the according mass loss of 0.05 wt% is too low to be detected in the TG measurement, as the hydride decomposition is overlapping with the second reduction step which starts already around 100 °C.<sup>49</sup>

The first optimized reduction procedure with a heating rate of 2 K/min and holding for 1 hour at 300 °C was used to investigate this second reduction step in more detail. The mass loss of 1.7(1) wt% in the second step during the optimized procedure correlates with the amount of oxygen, which has to be removed to obtain indium in an equimolar amount to palladium present in the sample. The calculated mass loss of 1.7 wt% perfectly fits the experimental result if one considers a palladium rich alloy to be formed after the first reduction step. This leads to the conclusion that InPd should be formed in the second reduction step, which was confirmed by subsequent XRD measurements (Figure 4).

The TPR is showing the next reduction step as a broad reduction peak around 350 °C. This third reduction step is characterized by a mass loss of 1.0(1) wt% during the reduction with a heating rate of 5 K/min and 1 hour holding time at 390 °C. The amount of reduced In<sub>2</sub>O<sub>3</sub> indicates that In<sub>3</sub>Pd<sub>2</sub> should be formed from the InPd ( $m_{\text{loss, calc}} = 1.1(1) \text{ wt\%}$ ), which is confirmed by XRD measurements of the reduced sample revealing only In<sub>3</sub>Pd<sub>2</sub> and In<sub>2</sub>O<sub>3</sub>. In the third optimized reduction procedure the PdO/In<sub>2</sub>O<sub>3</sub> was heated with 5 K/min and held at 550 °C for 3 hours. The mass loss of 11.4(1) wt%, thus the amount of reduced In<sub>2</sub>O<sub>3</sub>, is significantly higher than expected (1.8 wt%) from the formation of the indium-richest intermetallic compound In<sub>7</sub>Pd<sub>3</sub>. In the TPR measurement the signal is staying above the baseline after the reduction peak at 470 °C (Fig. 3).

An additional TPR measurement of single-phase In<sub>2</sub>O<sub>3</sub> revealed that the oxide is reduced to elemental indium in absence of palladium above 350 °C. Since the formation of In<sub>7</sub>Pd<sub>3</sub> needs higher temperatures this intermetallic compound can only be obtained in admixture with elemental indium. XRD patterns of the sample after reduction prove this hypothesis (Figure 4). Since thermodynamic data for the observed species involved in the reaction sequence for the formation of the In-Pd intermetallic compounds are available (Tab. S1), the Gibbs energy of each step starting from PdO/In<sub>2</sub>O<sub>3</sub> can be calculated according to eq. 6.

$$\Delta G = \Delta H^{\ominus} + \int_{298\text{ K}}^T c_p dT - T \left( \Delta S^{\ominus} + \int_{298\text{ K}}^T \frac{c_p}{T} dT \right) \quad \text{eq. (6)}$$

Interestingly, the results show that the most Pd-rich phase which should form under reaction conditions (i.e.  $\Delta G < 0$ ) is the alloy In<sub>17</sub>Pd<sub>83</sub> (see Supporting Information). For all other reactions, leading to intermetallic compounds, the Gibbs energy stays positive at least up to temperatures of 750 °C (Fig. S7). Thus the calculations indicate that additional species have to be considered, most likely activated hydrogen on the surface of the intermetallic compounds. The activation of the hydrogen and subsequent spill-over to the In<sub>2</sub>O<sub>3</sub> would most likely lead to lower Gibbs energies, but can not be considered here due to the lack of data.

Due to the strong reduction only 4 wt% of the In<sub>2</sub>O<sub>3</sub> support remain after reduction at 550 °C, resulting in a diminished surface area of the support. As a result, easier sintering of the particles is expected, which is in line with the increasing crystallite size of the intermetallic compounds (Table 2).

Table 2: Phase analysis and crystallite size of the intermetallic compounds after reductive treatment.

reductive treatment	sample composition	crystallite size
---------------------	--------------------	------------------

20 °C → 300 °C, 2 K/min, 1 h hold	InPd + In <sub>2</sub> O <sub>3</sub>	84 nm
20 °C → 390 °C, 5 K/min, 1 h hold	In <sub>3</sub> Pd <sub>2</sub> + In <sub>2</sub> O <sub>3</sub>	90 nm
20 °C → 550 °C, 5 K/min, 3 h hold	In <sub>7</sub> Pd <sub>3</sub> + In + In <sub>2</sub> O <sub>3</sub>	104 nm

### 3.2 Catalytic testing

The specific activity obtained by the catalytic measurement in the fixed-bed flow reactor for all tested materials is shown in Figure 5a. All materials had to be tested in MSR below their respective pre-reduction temperature to avoid the formation of additional intermetallic compounds, i.e. the InPd/In<sub>2</sub>O<sub>3</sub> sample could only be tested up to 300 °C. In the tested temperature range all materials showed an increase in their respective methanol steam reforming activity with increasing temperature. The intermetallic In-Pd compounds showed a decrease in the specific mass activity with increasing indium content. InPd exhibits a specific activity of 0.22  $\frac{\text{mmol MeOH}}{\text{mmol Pd} \cdot \text{h}}$  at 260 °C whereas In<sub>3</sub>Pd<sub>2</sub>/In<sub>2</sub>O<sub>3</sub> shows 0.12 and In<sub>7</sub>Pd<sub>3</sub> only 0.04  $\frac{\text{mmol MeOH}}{\text{mmol Pd} \cdot \text{h}}$  activity under the same reaction conditions. The supported intermetallic In-Pd compounds showed lower activity compared to the conventional Cu/ZnO/Al<sub>2</sub>O<sub>3</sub> sample, which exhibited a high specific activity of 1.1  $\frac{\text{mmol MeOH}}{\text{mmol Cu} \cdot \text{h}}$  (260 °C). The highest activity of 2.7  $\frac{\text{mmol MeOH}}{\text{mmol Pd} \cdot \text{h}}$  (260 °C) could be achieved with the Pd/SiO<sub>2</sub> sample on which no intermetallic compound formation occurs at the applied reaction conditions.<sup>22</sup>

A high selectivity is the most important benchmark for a good methanol steam reforming catalyst since CO formation has to be avoided. For a reliable comparison, the CO<sub>2</sub>-selectivity is always discussed at 30% methanol conversion (Figure 5b). All In-Pd/In<sub>2</sub>O<sub>3</sub> samples show a very high selectivity for methanol steam reforming. InPd/In<sub>2</sub>O<sub>3</sub> exhibits 91% selectivity to CO<sub>2</sub> at 260 °C,

while  $\text{In}_3\text{Pd}_2$  and  $\text{In}_7\text{Pd}_3$  reach selectivities of up to 98% at 260 °C. With increasing temperature the  $\text{CO}_2$ -selectivity is decreasing which can either be caused by reverse water gas shift (rWGS) or by methanol decomposition. All tested materials show  $\text{CO}_2$ -selectivities above the thermodynamic equilibrium (Figure 5b). Penner *et al.* showed that  $\text{In}_2\text{O}_3$  is not rWGS-active,<sup>50-51</sup> leaving the metallic surfaces as source for the CO. The copper catalyst shows a steep decrease in selectivity with temperature being caused by the rWGS activity of this material.<sup>52-53</sup> The  $\text{CO}_2$ -selectivity is dropping from 96.3% at 260 °C to 81.7% at 350 °C. The selectivity of the intermetallic In-Pd compounds is less affected by temperature, indicating a much lower rWGS activity. Especially the selectivities of  $\text{In}_3\text{Pd}_2$  and  $\text{In}_7\text{Pd}_3 + \text{In}$  only decrease by 6% in the measured temperature range. In contrast to the other tested materials,  $\text{Pd}/\text{SiO}_2$  shows nearly complete selectivity for methanol decomposition (only 2-5 %  $\text{CO}_2$  selectivity) in accordance to literature.<sup>19</sup> Thus, the high selectivity of the supported In-Pd/ $\text{In}_2\text{O}_3$  materials excludes the presence of elemental Pd.

From the specific activity a formal conversion rate could be determined and plotted as  $\ln k$  versus  $1/T$  to obtain an Arrhenius plot (Figure S1). Table 3 summarizes the derived apparent activation energies for the tested materials.

Table 3: Catalytic activity and selectivity at 260 °C and the derived apparent activation energies.

Sample	activity	selectivity [%]	$E_A$ [kJ/mol]	
	$\frac{[\text{mmol MeOH}]}{[\text{mmol Pd} \cdot \text{h}]}$		measured	literature
$\text{Pd}/\text{SiO}_2$	2.7	4.7	65(6)	-
$\text{InPd}/\text{In}_2\text{O}_3$	0.22	91.0	58(5)	61-64 <sup>23, 36</sup>
$\text{In}_3\text{Pd}_2/\text{In}_2\text{O}_3$	0.12	98.0	55(5)	
$(\text{In}_7\text{Pd}_3 + \text{In})/\text{In}_2\text{O}_3$	0.04	98.0	72(5)	
$\text{In}_2\text{O}_3$	-	-	-	98 <sup>51</sup>

Rameshan *et al.*<sup>36</sup> found an apparent activation energy of ~61 kJ/mol for a near-surface intermetallic In-Pd phase (NSIP) which is in good agreement with values determined for supported InPd (58(5) kJ/mol) and In<sub>3</sub>Pd<sub>2</sub> (55(5) kJ/mol). Lorenz *et al.*<sup>23</sup> also derived an apparent activation energy of ~64 kJ/mol for InPd/In<sub>2</sub>O<sub>3</sub>, which is comparable to our results. When they reduced their supported sample at temperatures above 300 °C they observed an In<sub>2</sub>O<sub>3</sub> layer encapsulating the intermetallic compound. The higher apparent activation energy for In<sub>7</sub>Pd<sub>3</sub>+In of 72(5) kJ/mol is likely caused by a similar effect. It can be assumed that the reduced indium is at least partly covering the In<sub>7</sub>Pd<sub>3</sub> particles influencing the catalytic properties of the intermetallic compound. This indium layer can then be easily oxidized under methanol steam reforming conditions as observed by XRD on the spent catalyst (see next section).

To show the potential of intermetallic In-Pd compounds as alternative to copper-based systems, catalytic long-term measurements of InPd/In<sub>2</sub>O<sub>3</sub> and Cu/ZnO/Al<sub>2</sub>O<sub>3</sub> over 100 hours time on stream at 260 °C were conducted (Figure 6). The conversion over the copper catalyst is decreasing exponentially with time on stream. In the beginning the Cu/ZnO/Al<sub>2</sub>O<sub>3</sub> catalyst converted 60% of the methanol decreasing to 10% after 100 hours. Although the significant decrease in the activity of the copper catalyst the selectivity for CO<sub>2</sub> stayed nearly constant at 97% over the whole measurement time. In contrast, the InPd/In<sub>2</sub>O<sub>3</sub> sample is activating over time so that in the beginning the sample had a methanol conversion of 40% which increased up to 50% after 100 hours time on stream. In addition, InPd/In<sub>2</sub>O<sub>3</sub> showed a significant increase in the selectivity for CO<sub>2</sub> from 87 to 93%. This observation implies that the sample changed during the catalytic testing over the long period which was confirmed by a XRD measurement of the sample after the long term measurement, revealing traces of In<sub>3</sub>Pd<sub>2</sub> besides InPd and In<sub>2</sub>O<sub>3</sub> (see next section). The formation of In<sub>3</sub>Pd<sub>2</sub> seems to be kinetically hindered since it could not

detected after the short term measurements of InPd/In<sub>2</sub>O<sub>3</sub>. It is known from ZnPd/ZnO that during MSR ZnO islands are formed on the surface of the intermetallic ZnPd particles which goes in hand with an increase of the activity and the selectivity of the supported material.<sup>34</sup> A subsequent reduction at elevated temperatures leads in this case to a decrease of the activity as well as the selectivity for the steam reforming reaction. After an additional hour time on stream the activity and selectivity are restored to the point prior the reduction.<sup>34</sup> In the case of ZnPd/ZnO interaction of the intermetallic ZnPd and the ZnO leads to an active and selective catalyst for MSR. Based on the catalytic data presented here, these processes could also explain the behavior of the InPd/In<sub>2</sub>O<sub>3</sub> system. In contrast to the ZnPd/ZnO system, a XRD measurement of the sample after the long term measurement revealed InPd and In<sub>2</sub>O<sub>3</sub> as main phases, but also traces of In<sub>3</sub>Pd<sub>2</sub>.

### 3.3 XRD after catalytic measurements

To investigate the stability during the steam reforming of methanol of the different In-Pd intermetallic compounds, XRD measurements of the samples were conducted after catalytic testing (Table 4).

Table 4: Sample composition (mol%) before and after catalytic measurements as determined by XRD.

	InPd / In <sub>2</sub> O <sub>3</sub>		In <sub>3</sub> Pd <sub>2</sub> / In <sub>2</sub> O <sub>3</sub>		In <sub>7</sub> Pd <sub>3</sub> +In / In <sub>2</sub> O <sub>3</sub>	
mol%	prior catalysis	after catalysis	prior catalysis	after catalysis	prior catalysis	after catalysis
In <sub>2</sub> O <sub>3</sub>	89.4	86.0	81.7	84.0	15.8	78.9

InPd	10.6	14.0	-	6.1	-	-
In <sub>3</sub> Pd <sub>2</sub>	-	-	18.3	9.9	-	16.5
In <sub>7</sub> Pd <sub>3</sub>	-	-	-	-	48.7	3.6
In	-	-	-	-	35.4	1.0

From the XRD analysis the InPd/In<sub>2</sub>O<sub>3</sub> sample is stable under MSR conditions. No traces of other intermetallic compounds or decomposition products are found after the catalytic measurement. Only the ratio of InPd:In<sub>2</sub>O<sub>3</sub> is changing during MSR. This is likely to be attributed to the reduction of In<sub>2</sub>O<sub>3</sub> and therefore a relative increase of the amount of InPd. In contrast, samples containing the indium richer compounds showed reflections of palladium-rich intermetallic compounds after the catalytic measurements. This indicates the high dynamics and adoptability of the intermetallic compounds to the applied atmosphere.

### 3.4 NAP XPS

Based on the results of the *ex situ* experiments, a reduction treatment up to 390 °C with 5 K/min in 0.5 mbar H<sub>2</sub> atmosphere was applied to obtain supported In-Pd intermetallic compounds starting from PdO/In<sub>2</sub>O<sub>3</sub>. The sample was in depth characterized by XPS before and after the reduction procedure (which was also monitored by NAP XPS) as well as under MSR conditions to investigate the changes occurring in the near-surface region *in operando*. The maximum temperature during MSR conditions was chosen 30 K below the respective reduction temperature to avoid formation of intermetallic compounds richer in indium. The results of the MS-measurements under in operando conditions are shown in **Figure S6**. MSR activity of the

supported materials was detected from 150 °C onwards increasing significantly with higher reaction temperatures.

In the as-prepared state (PdO/In<sub>2</sub>O<sub>3</sub>) under UHV conditions, the Pd3d signal consists of two different palladium species (Figure S2). According to literature, the Pd3d<sub>5/2</sub> signal at 337.3 eV is ascribed to PdO and the shoulder of the signal at 335.8 eV indicates the presence of elemental Pd.<sup>54-55</sup> The small shift of the signals compared to literature is likely to be attributed to partial charging of the sample during XPS measurement. Since the results of the *ex situ* investigations are pointing towards a full oxidation of the palladium, the small amount of elemental palladium might result from reduction by photoelectrons during the measurement. For the In3d signal only one species was detected (Figure S3). The position of the In3d<sub>5/2</sub> signal at 444.6 eV fits to the position of oxidic indium.<sup>56</sup> The indium-to-palladium ratio prior to reduction is approximately 2. In the as-prepared state the valence band (Fig. S5) is dominated by a high intensity at 3.1 eV, which can mainly be assigned to the Pd4d signal from PdO.<sup>57-58</sup> During reduction the maximum of the valence band shifts towards higher binding energies (4.0 eV). This shift of the signal can be assigned to the formation of intermetallic In-Pd compounds, which is in good agreement with literature.<sup>58</sup> During methanol steam reforming the valence band is dominated by In<sub>2</sub>O<sub>3</sub>, which can be explained by a coverage of the intermetallic particles with oxidic indium.<sup>59-60</sup> The In-Pd ratio of the near-surface region for the respective treatment is shown in Figure 7. In the as-prepared state the In/Pd ratio is 2 for all measured information depths. During synthesis the palladium is deposited on the surface of the In<sub>2</sub>O<sub>3</sub> support. During reduction the relative amount of indium is increasing leading to a In/Pd ratio of 4 (832 eV) up to 7 (232 eV). This increase can be explained with the formation of intermetallic In-Pd compounds and the diffusion of palladium into the bulk of the samples. During MSR conditions the relative In/Pd ratio is increasing

drastically leading to a ratio of 60 (832 eV) up to 105 (232 eV). Under steam reforming conditions the indium is segregating on the surface of the materials and forming oxidic species, covering the intermetallic particles. Depth-dependent measurements reveal a decreasing relative concentration of the carbon C1s signal with higher information depth indicating the presence of carbon only on the surface, resulting from the hydrocarbon background in the chamber.

Furthermore there is no hint on any C1s species connected to subsurface carbon.<sup>61</sup> Since for all measurements subsurface carbon could be excluded the carbon signal will not be discussed any further.

Changes occurring to the Pd3d<sub>5/2</sub> signal during the reduction of the samples up to 390 °C were recorded *in situ* with a kinetic energy of 532 eV corresponding to an information depth of 3.2 nm (Figure 8). At room temperature PdO is readily reduced to elemental Pd which is seen by the depletion of the Pd3d<sub>5/2</sub> signal at 337.3 eV and increasing intensity of the signal at 335.3 eV.

Although the peak position is shifted to higher binding energies compared to bulk Pd the asymmetric shape and the relative shift of the Pd3d signal proof this assignment. It is again quite likely that the small shift is caused by partial charging of the sample. At approximately 150 °C – after full reduction of PdO – the maximum of the Pd3d<sub>5/2</sub> signal starts to shift during further reduction to higher binding energies up to 336.5 eV. Above 300 °C no further shift of the Pd3d<sub>5/2</sub> signal is observed. The shift of the Pd signal can be explained by the formation of intermetallic In-Pd compounds which agrees with earlier results.<sup>36</sup> Furthermore, the signal intensity is reduced significantly upon formation of the intermetallic compounds, which is related to the depleted Pd concentration in the near-surface region due to the presence of indium in the intermetallic compounds. Upon reduction up to 390 °C the palladium content in the near-surface region is decreasing to 2-5 at% compared to ~10 at% in the as prepared state. The amount of oxygen

within the near-surface region of the sample is not affected (not shown). In line with the formation of intermetallic compounds, the concentration of indium in the near-surface region increased during reduction. After the reduction, only intermetallic palladium could be observed in the Pd3d spectra. Concerning the In3d spectra (Figure S3), the signal – representing a combination of all different indium species – is shifted to lower binding energies and became asymmetric during the reductive treatment. Since intermetallic indium exhibits a lower binding energy compared to oxidic indium,<sup>36</sup> the shift is also in accordance with the formation of In-Pd intermetallic compounds.

Although during methanol steam reforming the total oxygen content in the near-surface region remains constant up to the maximum temperature of 360 °C oxidic species are changing. Due to the high influence of the support the different species can not be discriminated from each other, which is the major drawback of the In-Pd/In<sub>2</sub>O<sub>3</sub> material. The position of the Pd3d<sub>5/2</sub> signal is not shifted (Figure 9). This proves that no elemental Pd or PdO has formed under reactive conditions. Only the intensity of the Pd signal decreased further compared to the reduced state, while the In3d signal became more pronounced, indicating segregation of indium species to the surface. Thus, during the *operando* measurement the surface becomes depleted in palladium. The In3d peak shape becomes symmetric again and the peak position changed back to the position of the as prepared state under MSR conditions. This indicates that a significant amount of the reduced indium got oxidized during MSR conditions. The indium to palladium ratio increases up to 100 during MSR, indicating that the intermetallic particles become nearly fully covered by oxidic indium.

Results from earlier grazing incidence X-ray diffraction experiments on polycrystalline In<sub>52</sub>Pd<sub>48</sub> under *operando* conditions show that near-surface In<sub>2</sub>O<sub>3</sub> gets easily reduced in hydrogen

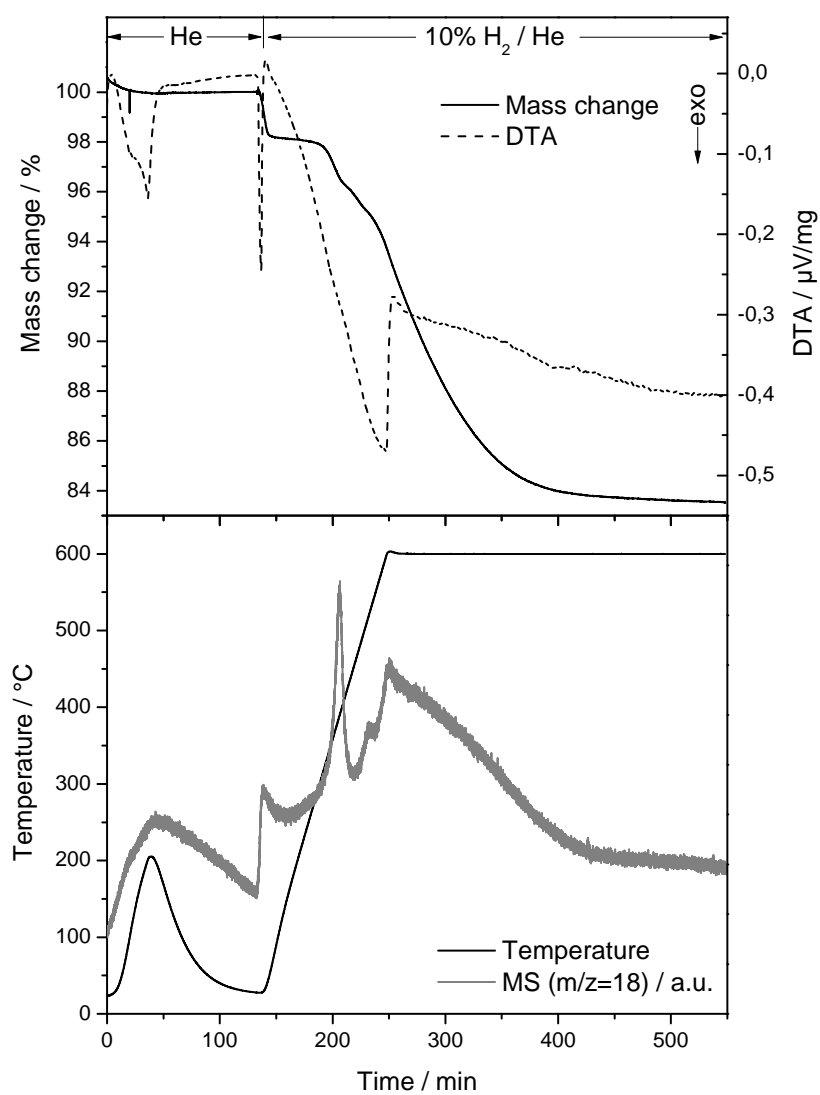
containing atmosphere.<sup>62</sup> The formed indium diffuses into the bulk and reacts with intermetallic In-Pd species forming indium-rich compounds. On the other hand, the surface of  $\text{In}_{52}\text{Pd}_{48}$  gets oxidized when steam reforming conditions are applied to the materials. Using surface sensitive X-ray diffraction experiments under grazing incident angle (GIXRD) the formation of  $\text{In}_2\text{O}_3$  on the surface of the unsupported intermetallic compound could be detected. The reactive atmosphere is not affecting the bulk of the  $\text{In}_{52}\text{Pd}_{48}$  sample. From the results obtained in this work it can be concluded that the unsupported and the supported materials show a similar behavior in hydrogen and under steam reforming conditions. A scheme summarizing the changes of the supported materials during reduction and catalytic measurement is shown in Figure 10.

#### 4 Conclusions

DTA/TG/MS is a very valuable combination of techniques to investigate the formation of intermetallic compounds. This is especially of importance if supported materials are used like in these investigations on  $\text{PdO}/\text{In}_2\text{O}_3$ . Through these measurements three separate procedures could be quickly developed which led to supported single-phase  $\text{InPd}$  and  $\text{In}_3\text{Pd}_2$  as well as  $\text{In}_7\text{Pd}_3$  in a mixture with elemental In. NAP XPS measurements showed that  $\text{PdO}$  is reduced to elemental Pd in hydrogen atmosphere already at room temperature, followed by the formation of intermetallic compounds above 150 °C. XRD and XPS measurements proved that no elemental Pd is present after the respective reduction procedure. Catalytic measurements in a fixed-bed flow reactor further proved the potential of the supported intermetallic compounds for the hydrogen production from methanol. All materials exhibit activity and a high selectivity for methanol steam reforming. Especially  $\text{In}_3\text{Pd}_2$  and  $\text{In}_7\text{Pd}_3$  showed  $\text{CO}_2$  selectivities above 98% at 30% methanol conversion. Although these compounds seem to decompose into the respective palladium-rich compounds and  $\text{In}_2\text{O}_3$ , these materials are interesting as precursor materials of a

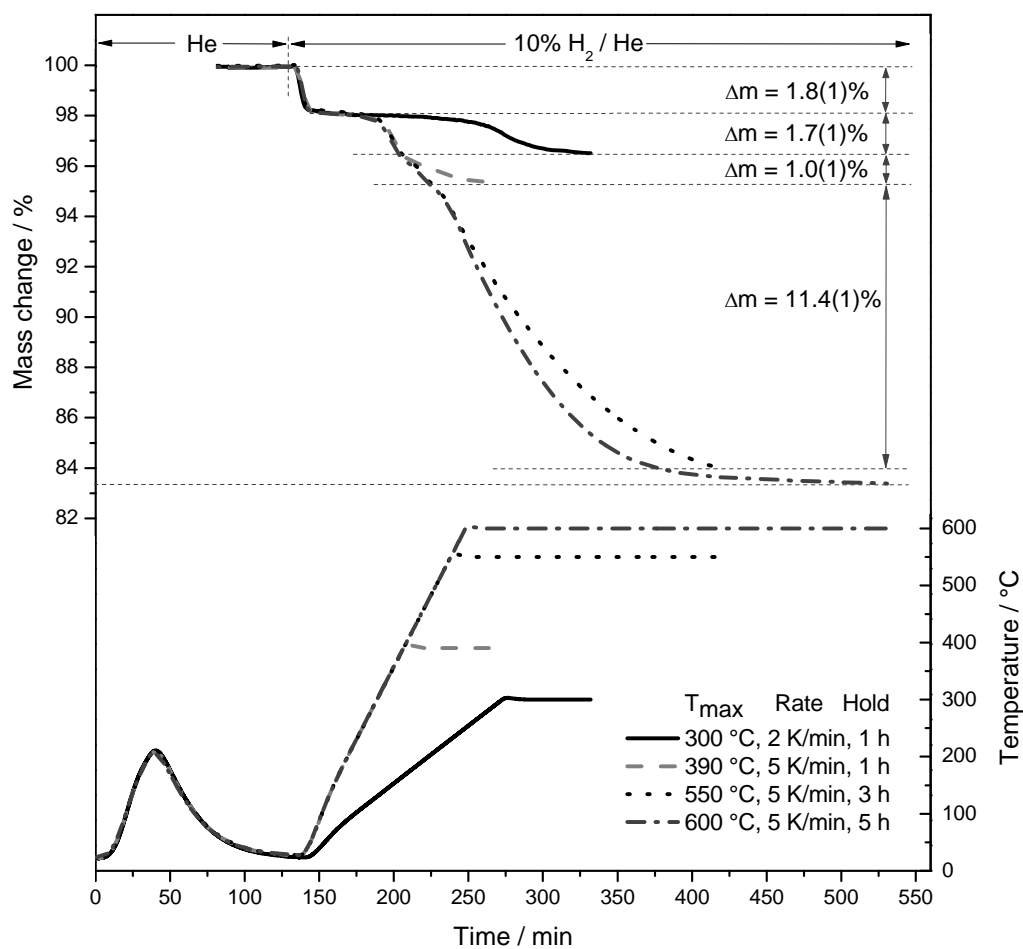
high selective methanol steam reforming catalyst. Because of the easy reduction of  $\text{In}_2\text{O}_3$ , a highly dynamic behavior of the supported materials could be observed. Besides the pretreatment, the reaction conditions and the conversion have a crucial impact on the changes of the materials. XPS investigations revealed that during methanol steam reforming the near-surface region of the supported  $\text{In-Pd}/\text{In}_2\text{O}_3$  becomes enriched in indium, which is partially oxidized. Although these materials are quite complex, long-term measurements with up to 100 hours time on stream proved the feasibility of  $\text{InPd}/\text{In}_2\text{O}_3$  as alternative to the common  $\text{Cu}/\text{ZnO}/\text{Al}_2\text{O}_3$  catalyst. The supported intermetallic  $\text{InPd}$  compound exhibited high activity and  $\text{CO}_2$ -selectivity and showed a high catalytic stability over the whole measurement time. In contrast, the copper catalyst deactivated relatively fast. Up to now it is not fully clarified how the selectivity in methanol steam reforming depends upon the respective  $\text{In-Pd}$  compound, requiring further investigations for a better understanding.

## FIGURES



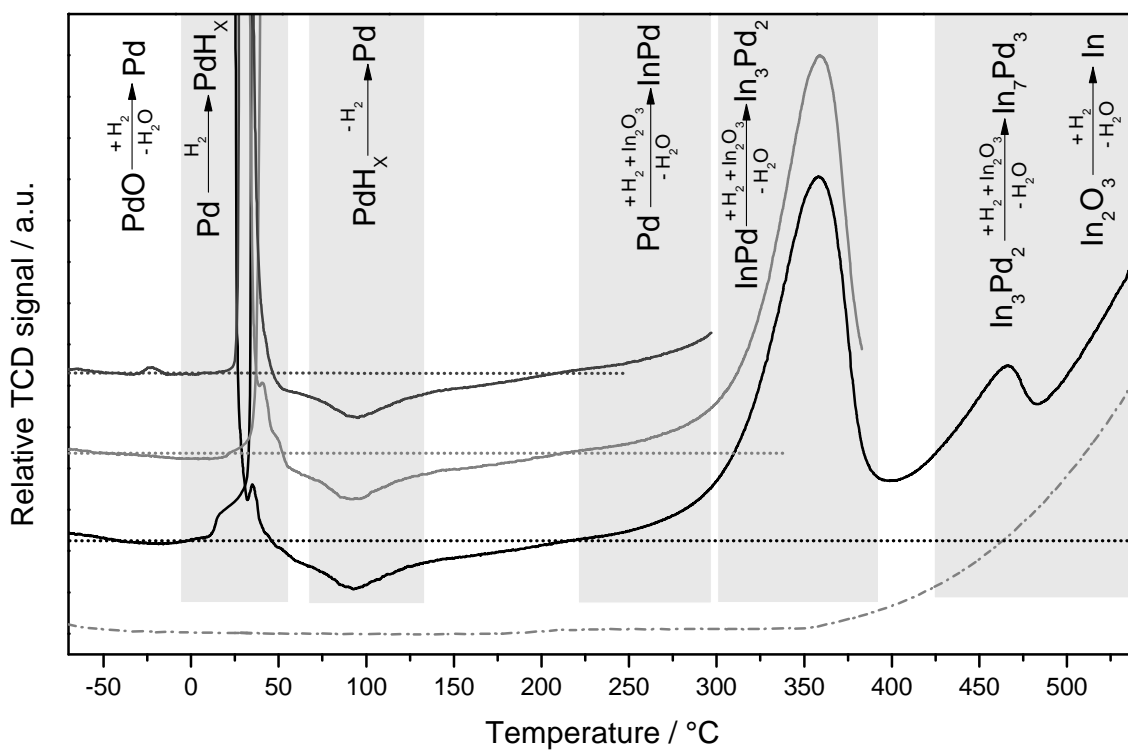
472

473 Figure 1: DTA/TG/MS measurement of  $\text{PdO}/\text{In}_2\text{O}_3$  in 10%  $\text{H}_2/\text{He}$  up to 600 °C with 5 K/min.



474

475 Figure 2: Comparison of the TG signals of PdO/In<sub>2</sub>O<sub>3</sub> with different temperature treatments.



476  
 477 Figure 3: TPR measurements of PdO/In<sub>2</sub>O<sub>3</sub> (solid lines) and In<sub>2</sub>O<sub>3</sub> (dashed line) with 5 K/min in  
 478 10 vol% H<sub>2</sub>/Ar.

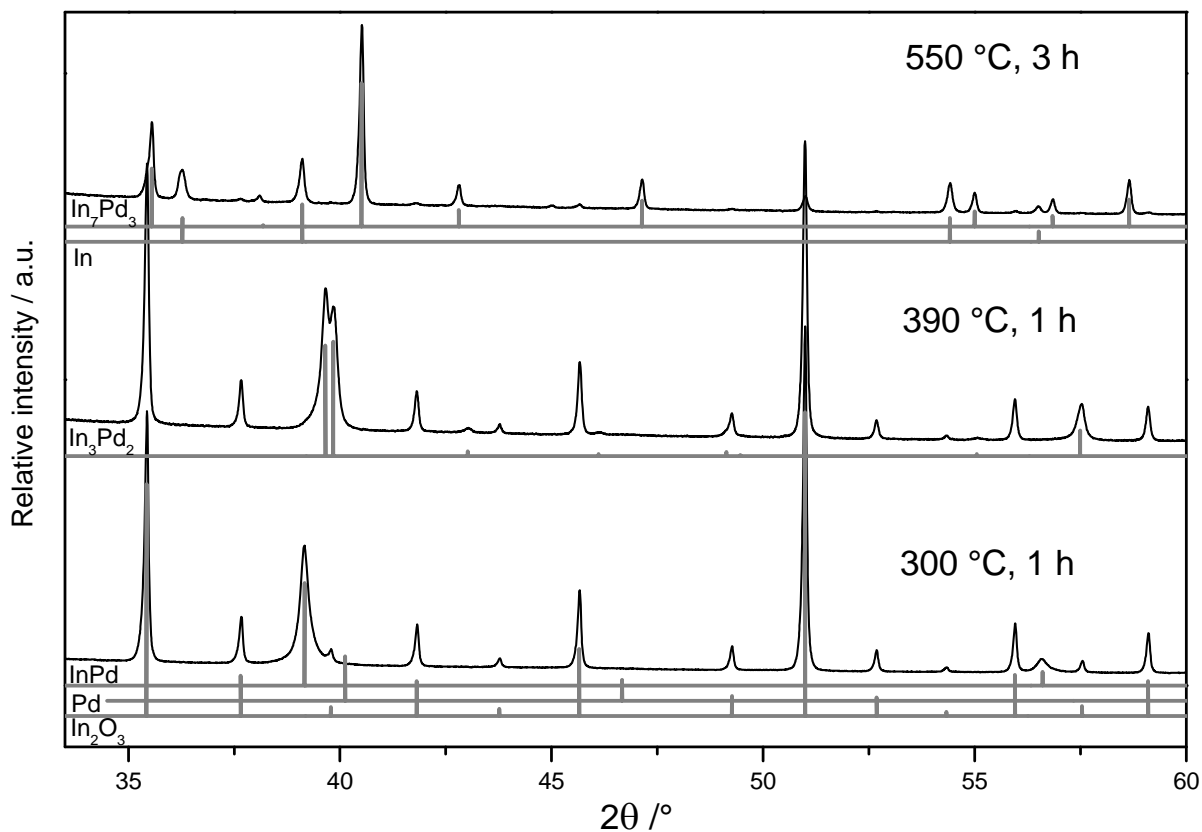
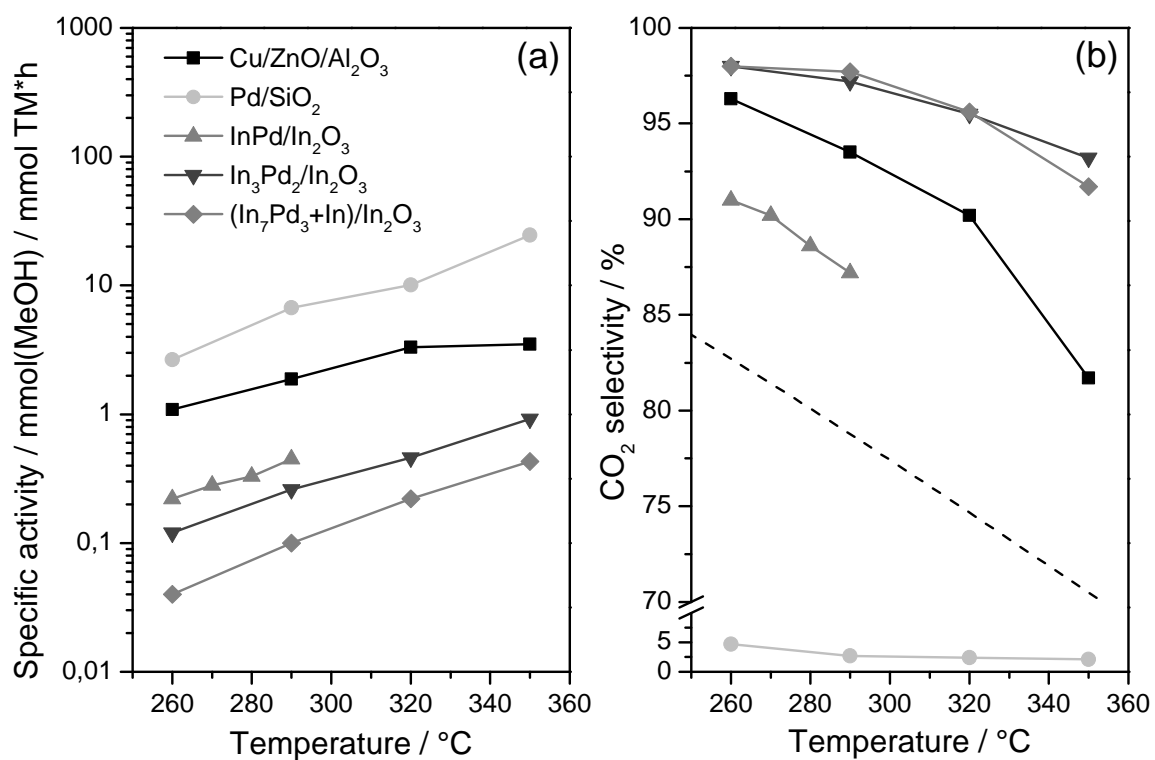


Figure 4: Powder X-ray diffraction patterns of PdO/In<sub>2</sub>O<sub>3</sub> after the indicated reductive treatments. Calculated diffraction patterns (In<sup>63</sup>, Pd<sup>64</sup>, In<sub>2</sub>O<sub>3</sub><sup>65</sup>, InPd<sup>66</sup>, In<sub>3</sub>Pd<sub>2</sub><sup>66</sup> and In<sub>7</sub>Pd<sub>3</sub><sup>67</sup>) are shown between the diffraction patterns.

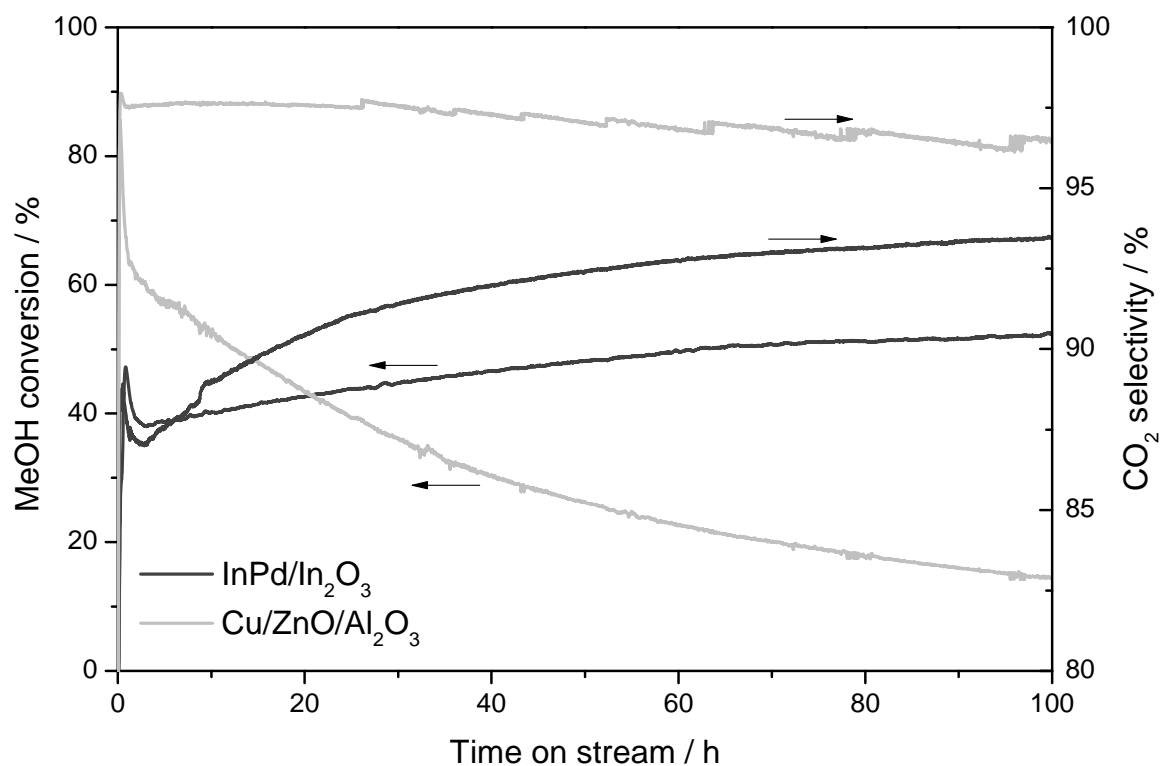


487

488 Figure 5: Specific MSR-activity per mmol transition metal (TM) (a) and CO<sub>2</sub> selectivity at 30%

489 methanol conversion of the tested materials (b). The dashed line indicates the CO<sub>2</sub>-selectivity in

490 thermodynamic equilibrium.



491  
 492 Figure 6: Long-term catalytic measurements for InPd/In<sub>2</sub>O<sub>3</sub> (3000 mg) and Cu/ZnO/Al<sub>2</sub>O<sub>3</sub> (100  
 493 mg) in methanol steam reforming at 260 °C.

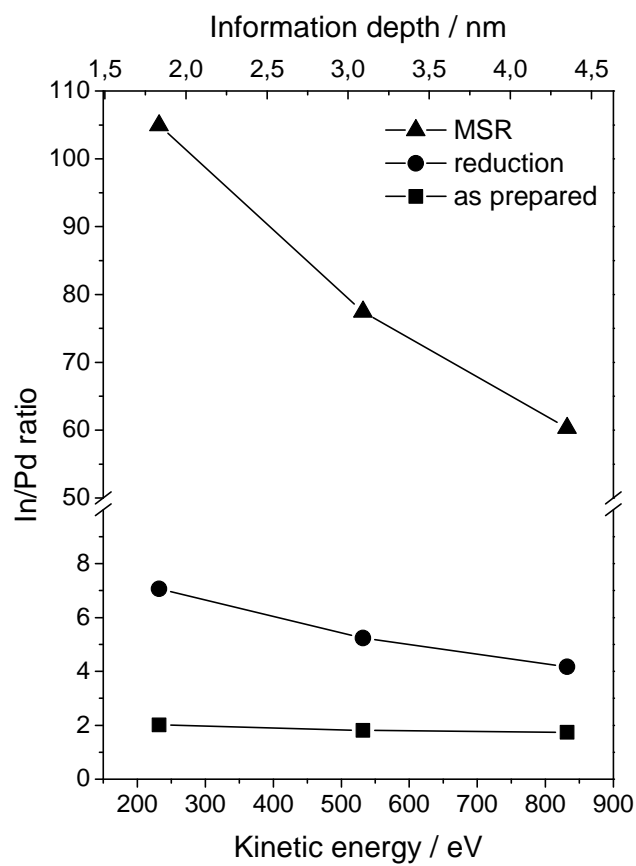
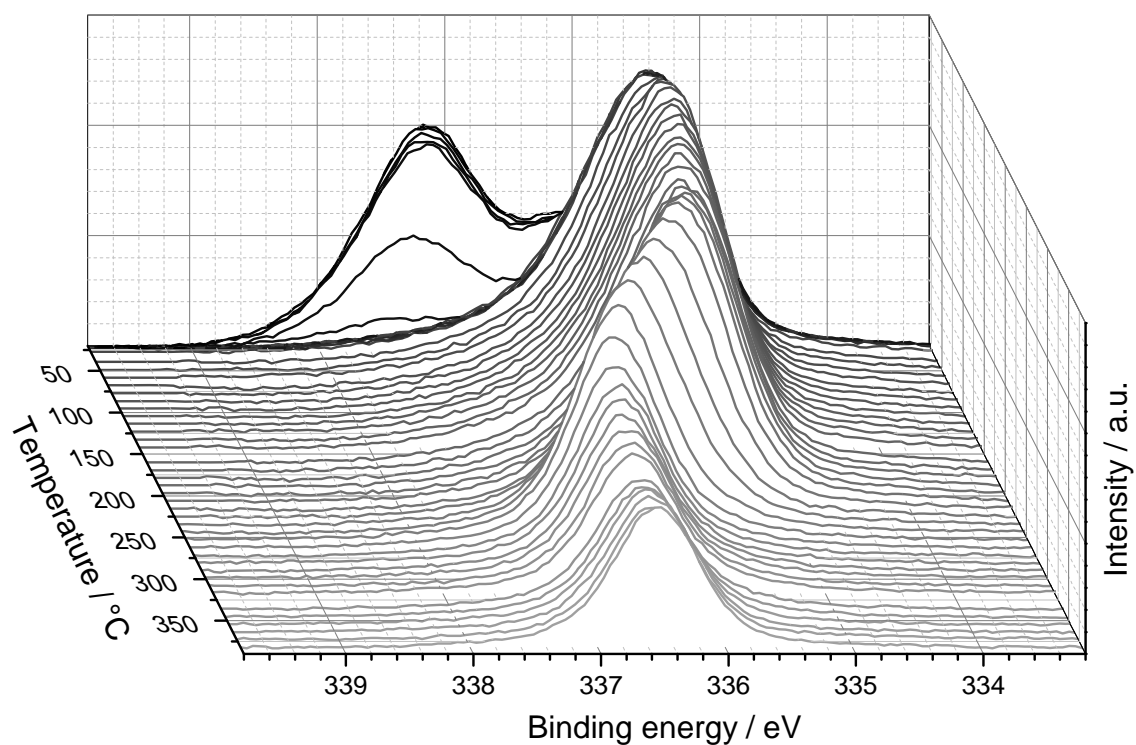


Figure 7: In-Pd ratio of PdO/In<sub>2</sub>O<sub>3</sub> in the near-surface region by XPS after different treatments.



498  
 499 Figure 8: The evolution of the Pd3d<sub>3/2</sub> signal during reduction of PdO/In<sub>2</sub>O<sub>3</sub> up to 390 °C  
 500 revealing the reduction of PdO to elemental palladium at ambient temperature and formation of  
 501 the In-Pd alloy and intermetallic compounds from 150 °C onward.  
 502

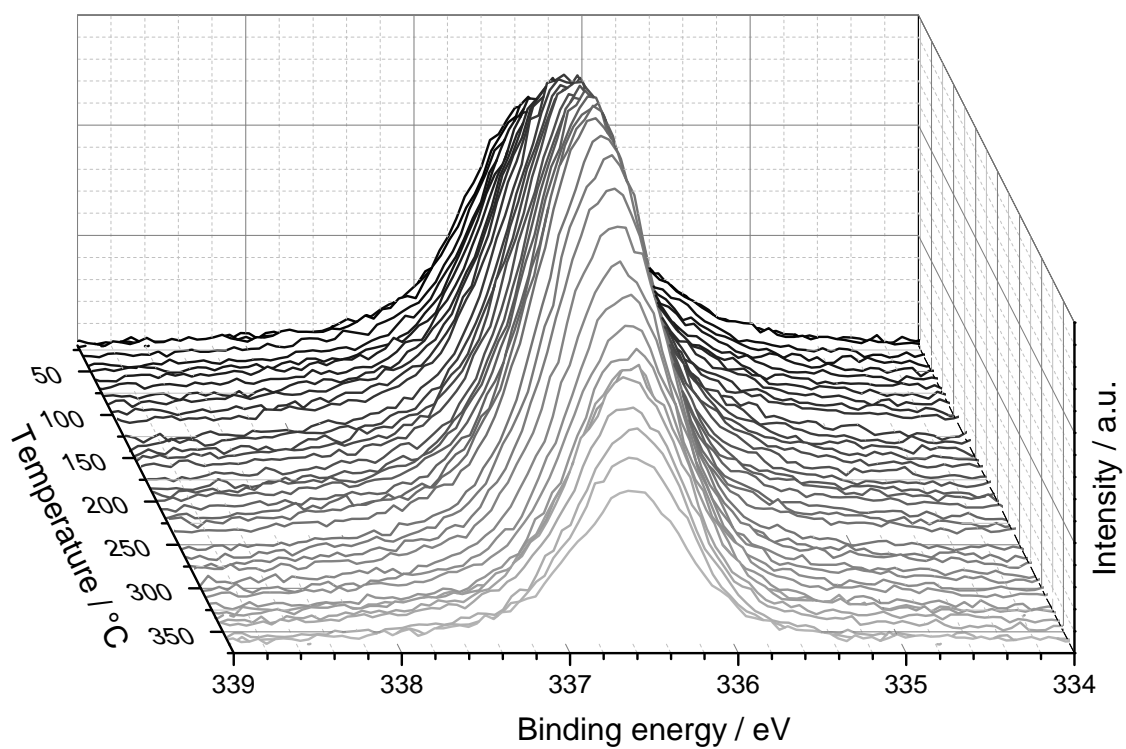


Figure 9: The evolution of the Pd $3d_{3/2}$  signal during MSR measurement of In-Pd/In $_2$ O $_3$  up to 360 °C.

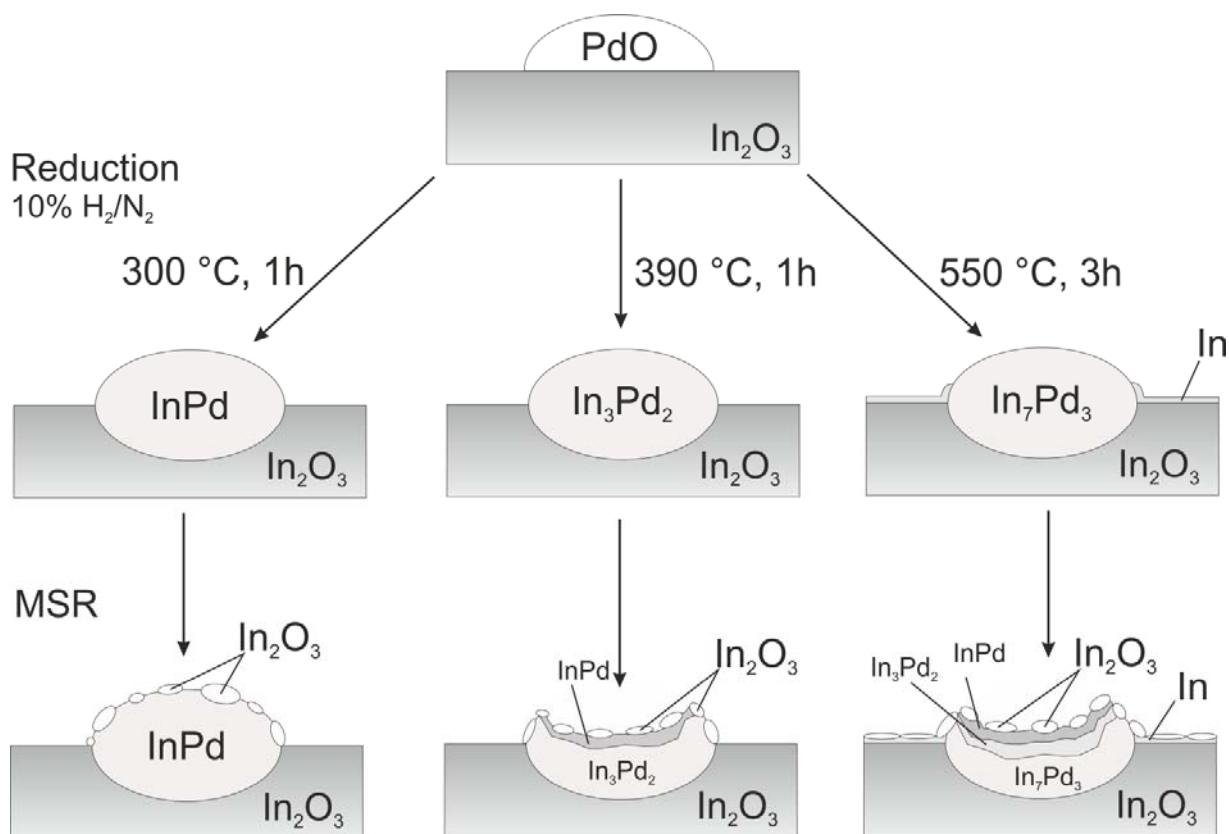
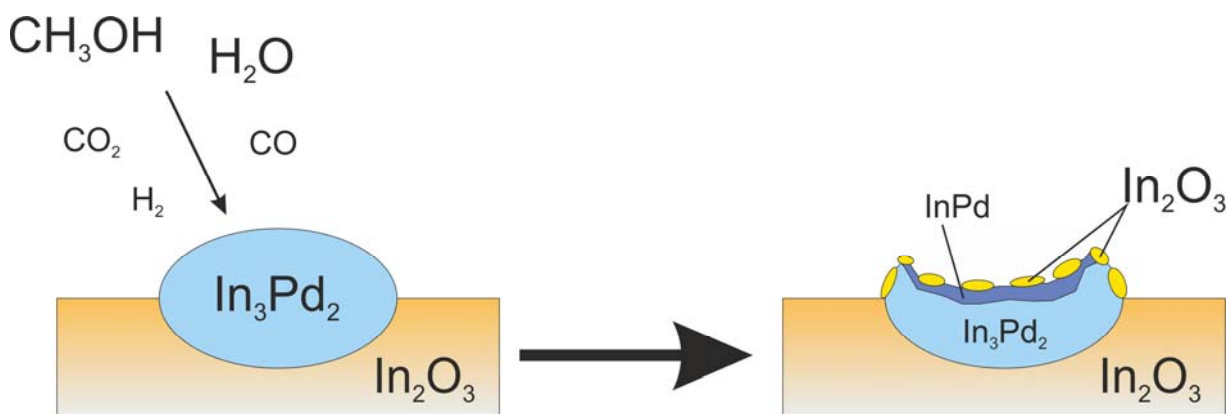


Figure 10: Scheme of chemical transformation of  $\text{PdO}/\text{In}_2\text{O}_3$  upon reduction and MSR.



518  
519  
520  
521  
  
522  
  
523  
524  
  
525  
  
526  
527  
  
528  
  
529  
530  
531  
532  
533  
534  
535  
536  
  
537  
538  
539

## AUTHOR INFORMATION

### **Corresponding Author**

\* M. Armbrüster, marc.armbruester@chemie.tu-chemnitz.de

### **Author Contributions**

The manuscript was written through contributions of all authors. All authors have given approval to the final version of the manuscript.

### **Funding Sources**

The authors thank the ‘Deutsche Forschungsgemeinschaft’ (DFG) for funding the investigations (project AR 617/5-1). Further support was gained through the COST Action CM0904.

## ACKNOWLEDGMENT

A. Zhang is acknowledged for the DTA/TG measurements. The authors thank M. Schmidt for his help and fruitful discussion on the thermodynamic calculations. H. Bormann is acknowledged for XRD measurements. Great thanks to M. Friedrich for his help with the XPS spectra and to G. Auffermann for the ICP-OES measurements. Wacker Chemie AG is acknowledged for providing a sample of HDK-N20. The authors thank the Helmholtz Zentrum Berlin für Materialien und Energie GmbH for beamtime at BESSY II. The authors thank the ‘Deutsche Forschungsgemeinschaft’ (DFG) for funding the investigations (project AR 617/5-1). Further support was gained through the COST Action CM0904.

## REFERENCES

- 540 1. Armaroli, N.; Balzani, V., The future of energy supply: Challenges and opportunities.  
541 *Angew. Chem., Int. Ed.* **2007**, *46* (1-2), 52-66.
- 542 2. Dincer, I.; Rosen, M. A., Sustainability aspects of hydrogen and fuel cell systems. *Energy*  
543 *Sustainable Dev.* **2011**, *15* (2), 137-146.
- 544 3. Eberle, U.; Felderhoff, M.; Schuth, F., Chemical and Physical Solutions for Hydrogen  
545 Storage. *Angew. Chem., Int. Ed.* **2009**, *48* (36), 6608-6630.
- 546 4. Schüth, F., Challenges in hydrogen storage. *Eur. Phys. J.: Spec. Top.* **2009**, *176*, 155-166.
- 547 5. Zerta, M.; Schmidt, P. R.; Stiller, C.; Landinger, H., Alternative World Energy Outlook  
548 (AWEO) and the role of hydrogen in a changing energy landscape. *Int. J. Hydrogen Energy*  
549 **2008**, *33* (12), 3021-3025.
- 550 6. Armaroli, N.; Balzani, V., The Hydrogen Issue. *ChemSusChem* **2011**, *4* (1), 21-36.
- 551 7. Neef, H. J., International overview of hydrogen and fuel cell research. *Energy* **2009**, *34*  
552 (3), 327-333.
- 553 8. Lemus, R. G.; Duarte, J. M. M., Updated hydrogen production costs and parities for  
554 conventional and renewable technologies. *Int. J. Hydrogen Energy* **2010**, *35* (9), 3929-3936.
- 555 9. Abe, R., Recent progress on photocatalytic and photoelectrochemical water splitting  
556 under visible light irradiation. *J. Photochem. Photobiol., C* **2010**, *11* (4), 179-209.
- 557 10. Minggu, L. J.; Daud, W. R. W.; Kassim, M. B., An overview of photocells and  
558 photoreactors for photoelectrochemical water splitting. *Int. J. Hydrogen Energy* **2010**, *35* (11),  
559 5233-5244.
- 560 11. Mazloomi, K.; Gomes, C., Hydrogen as an energy carrier: Prospects and challenges.  
561 *Renewable Sustainable Energy Rev.* **2012**, *16* (5), 3024-3033.
- 562 12. Jena, P., Materials for Hydrogen Storage: Past, Present, and Future. *J. Phys. Chem. Lett.*  
563 **2011**, *2* (3), 206-211.
- 564 13. Schüth, F., Chemical Compounds for Energy Storage. *Chem. Ing. Tech.* **2011**, *83* (11),  
565 1984-1993.
- 566 14. Von Burg, R., Methanol. *J. Appl. Toxicol.* **1994**, *14* (4), 309-313.
- 567 15. Gasoline. *J. Appl. Toxicol.* **1989**, *9* (3), 203-210.
- 568 16. Behrens, M.; Armbrüster, M., Methanol Steam Reforming. In *Catalysis for Alternative*  
569 *Energy Generation*, Guczi, L.; Erdohelyi, A., Eds. Springer: **2012**, 175-235.
- 570 17. Oetjen, H. F.; Schmidt, V. M.; Stimming, U.; Trila, F., Performance data of a proton  
571 exchange membrane fuel cell using H<sub>2</sub>/CO as fuel gas. *J. Electrochem. Soc.* **1996**, *143* (12),  
572 3838-3842.
- 573 18. Kurtz, M.; Wilmer, H.; Genger, T.; Hinrichsen, O.; Muhler, M., Deactivation of  
574 supported copper catalysts for methanol synthesis. *Catal. Lett.* **2003**, *86* (1-3), 77-80.
- 575 19. Iwasa, N.; Kudo, S.; Takahashi, H.; Masuda, S.; Takezawa, N., Highly Selective  
576 Supported Pd Catalysts for Steam Reforming of Methanol. *Catal. Lett.* **1993**, *19* (2-3), 211-216.
- 577 20. Iwasa, N.; Mayanagi, T.; Ogawa, N.; Sakata, K.; Takezawa, N., New catalytic functions  
578 of Pd-Zn, Pd-Ga, Pd-In, Pt-Zn, Pt-Ga and Pt-In alloys in the conversions of methanol. *Catal.*  
579 *Lett.* **1998**, *54* (3), 119-123.
- 580 21. Iwasa, N.; Yamamoto, O.; Tamura, R.; Nishikubo, M.; Takezawa, N., Difference in the  
581 reactivity of acetaldehyde intermediates in the dehydrogenation of ethanol over supported Pd  
582 catalysts. *Catal. Lett.* **1999**, *62* (2-4), 179-184.
- 583 22. Penner, S.; Armbrüster, M., Formation of Intermetallic Compounds by Reactive Metal-  
584 Support Interaction: A Frequently Encountered Phenomenon in Catalysis. *ChemCatChem* **2015**,  
585 *7* (3), 374-392.

23. Lorenz, H.; Turner, S.; Lebedev, O. I.; Van Tendeloo, G.; Klötzer, B.; Rameshan, C.; Pfaller, K.; Penner, S., Pd-In<sub>2</sub>O<sub>3</sub> interaction due to reduction in hydrogen: Consequences for methanol steam reforming. *Appl. Catal., A* **2010**, *374* (1-2), 180-188.
24. Marchesini, F. A.; Irusta, S.; Querini, C.; Miro, E., Spectroscopic and catalytic characterization of Pd-In and Pt-In supported on Al<sub>2</sub>O<sub>3</sub> and SiO<sub>2</sub>, active catalysts for nitrate hydrogenation. *Appl. Catal., A* **2008**, *348* (1), 60-70.
25. Men, Y.; Kolb, G.; Zapf, R.; O'Connell, M.; Ziogas, A., Methanol steam reforming over bimetallic Pd-In/Al<sub>2</sub>O<sub>3</sub> catalysts in a microstructured reactor. *Appl. Catal., A* **2010**, *380* (1-2), 15-20.
26. Umegaki, T.; Yamada, Y.; Ueda, A.; Kuriyama, N.; Xu, Q., Hydrogen Production via Steam Reforming of Ethyl Alcohol over Palladium/Indium Oxide Catalyst. *Adv. Phys. Chem.* **2009**, *2009*, 1-4.
27. Wencka, M.; Hahne, M.; Kocjan, A.; Vrtnik, S.; Koželj, P.; Korže, D.; Jagličić, Z.; Sorić, M.; Popčević, P.; Ivkov, J.; Smontara, A.; Gille, P.; Jurga, S.; Tomeš, P.; Paschen, S.; Ormeci, A.; Armbrüster, M.; Grin, Y.; Dolinšek, J., Physical properties of the InPd intermetallic catalyst. *Intermetallics* **2014**, *55* (0), 56-65.
28. Valdes-Solis, T.; Marban, G.; Fuertes, A. B., Nanosized catalysts for the production of hydrogen by methanol steam reforming. *Catal. Today* **2006**, *116* (3), 354-360.
29. Sa, S.; Silva, H.; Brandao, L.; Sousa, J. M.; Mendes, A., Catalysts for methanol steam reforming-A review. *Appl. Catal., B* **2010**, *99* (1-2), 43-57.
30. Armbrüster, M.; Behrens, M.; Föttinger, K.; Friedrich, M.; Gaudry, É.; Matam, S. K.; Sharma, H. R., The Intermetallic Compound ZnPd and Its Role in Methanol Steam Reforming. *Catal. Rev.* **2013**, *55* (3), 289-367.
31. Friedrich, M.; Teschner, D.; Knop-Gericke, A.; Armbrüster, M., Influence of bulk composition of the intermetallic compound ZnPd on surface composition and methanol steam reforming properties. *J. Catal.* **2012**, *285* (1), 41-47.
32. Lorenz, H.; Friedrich, M.; Armbrüster, M.; Klotzer, B.; Penner, S., ZnO is a CO<sub>2</sub>-selective steam reforming catalyst. *J. Catal.* **2013**, *297* (C), 151-154.
33. Penner, S.; Jenewein, B.; Gabasch, H.; Klötzer, B.; Wang, D.; Knop-Gericke, A.; Schlögl, R.; Hayek, K., Growth and structural stability of well-ordered PdZn alloy nanoparticles. *J. Catal.* **2006**, *241* (1), 14-19.
34. Friedrich, M.; Penner, S.; Heggen, M.; Armbrüster, M., High CO<sub>2</sub> Selectivity in Methanol Steam Reforming through ZnPd/ZnO Teamwork. *Angew. Chem., Int. Ed.* **2013**, *52* (16), 4389-4392.
35. Iwasa, N.; Takezawa, N., New supported Pd and Pt alloy catalysts for steam reforming and dehydrogenation of methanol. *Top. Catal.* **2003**, *22* (3-4), 215-224.
36. Rameshan, C.; Lorenz, H.; Mayr, L.; Penner, S.; Zemlyanov, D.; Arrigo, R.; Hävecker, M.; Blume, R.; Knop-Gericke, A.; Schlögl, R.; Klötzer, B., CO<sub>2</sub>-selective methanol steam reforming on In-doped Pd studied by in situ X-ray photoelectron spectroscopy. *J. Catal.* **2012**, *295* (0), 186-194.
37. Lorenz, B.; Montini, T.; De Rogatis, L.; Canton, P.; Benedetti, A.; Fornasiero, P., Hydrogen production through alcohol steam reforming on Cu/ZnO-based catalysts. *Appl. Catal., B* **2011**, *101* (3-4), 397-408.
38. *PowderCell 2.4*, Bundesanstalt für Materialforschung und -prüfung, **2000**.
39. Knop-Gericke, A.; Kleimenov, E.; Hävecker, M.; Blume, R.; Teschner, D.; Zafeirotas, S.; Schlögl, R.; Bukhtiyarov, V. I.; Kaichev, V. V.; Prosvirin, I. P.; Nizovskii, A. I.; Bluhm, H.

Barinov, A.; Dudin, P.; Kiskinova, M., X-Ray Photoelectron Spectroscopy for Investigation of Heterogeneous Catalytic Processes. In *Adv. Catal.*, Academic Press: **2009**, 52, 213-272.

40. Seah, M. P., An accurate and simple universal curve for the energy-dependent electron inelastic mean free path. *Surf. Interface Anal.* **2012**, 44 (4), 497-503.

41. Evans, S., Correction for the effects of adventitious carbon overlayers in quantitative XPS analysis. *Surf. Interface Anal.* **1997**, 25 (12), 924-930.

42. *CasaXPS Version 2.3.16*, **2010**.

43. Shirley, D. A., High-Resolution X-Ray Photoemission Spectrum of the Valence Bands of Gold. *Phys. Rev. B* **1972**, 5 (12), 4709-4714.

44. Lindau, I.; Yeh, J. J., Atomic Subshell Photoionization Cross Sections and Asymmetry Parameters:  $1 < Z < 103$ . *At. Data Nucl. Data Tables* **1985**, 32, 1-155.

45. Okamoto, H., In-Pd (Indium-Palladium). *J. Phase Equilib.* **2003**, 24 (5), 481-481.

46. Kohlmann, H., Hydrogenation of palladium rich compounds of aluminium, gallium and indium. *J. Solid State Chem.* **2010**, 183 (2), 367-372.

47. Maier, W. F. 11th Conference on the Catalysis of Organic Reactions, Savannah, Rylander, P. N.; Greenfield, H.; Augustine, R. L., Eds. Marcel Dekker Inc: Savannah, 1986.

48. Jenewein, B.; Penner, S.; Gabasch, H.; Klötzer, B.; Wang, D.; Knop-Gericke, A.; Schlögl, R.; Hayek, K., Hydride formation and stability on a Pd-SiO<sub>2</sub> thin-film model catalyst studied by TEM and SAED. *J. Catal.* **2006**, 241 (1), 155-161.

49. Iwasa, N.; Mayanagi, T.; Nomura, W.; Arai, M.; Takezawa, N., Effect of Zn addition to supported Pd catalysts in the steam reforming of methanol. *Appl. Catal., A* **2003**, 248 (1-2), 153-160.

50. Bielz, T.; Lorenz, H.; Amann, P.; Klötzer, B.; Penner, S., Water-Gas Shift and Formaldehyde Reforming Activity Determined by Defect Chemistry of Polycrystalline In<sub>2</sub>O<sub>3</sub>. *J. Phys. Chem. C* **2011**, 115 (14), 6622-6628.

51. Lorenz, H.; Jochum, W.; Klötzer, B.; Stöger-Pollach, M.; Schwarz, S.; Pfaller, K.; Penner, S., Novel methanol steam reforming activity and selectivity of pure In<sub>2</sub>O<sub>3</sub>. *Appl. Catal., A* **2008**, 347 (1), 34-42.

52. Purnama, H.; Ressler, T.; Jentoft, R. E.; Soerijanto, H.; Schlögl, R.; Schomäcker, R., CO formation/selectivity for steam reforming of methanol with a commercial CuO/ZnO/Al<sub>2</sub>O<sub>3</sub> catalyst. *Appl. Catal., A* **2004**, 259 (1), 83-94.

53. Sa, S.; Sousa, J. M.; Mendes, A., Steam reforming of methanol over a CuO/ZnO/Al<sub>2</sub>O<sub>3</sub> catalyst, part I: Kinetic modelling. *Chem. Eng. Sci.* **2011**, 66 (20), 4913-4921.

54. Militello, M. C.; Simko, S. J., Elemental Palladium by XPS. *Surf. Sci. Spectra* **1994**, 3 (4), 387-394.

55. Militello, M. C.; Simko, S. J., Palladium Oxide (PdO) by XPS. *Surf. Sci. Spectra* **1994**, 3 (4), 395-401.

56. Faur, M.; Faur, M.; Jayne, D. T.; Goradia, M.; Goradia, C., XPS investigation of anodic oxides grown on p-type InP. *Surf. Interface Anal.* **1990**, 15 (11), 641-650.

57. Brun, M.; Berthet, A.; Bertolini, J. C., XPS, AES and Auger parameter of Pd and PdO. *J. Electron Spectrosc. Relat. Phenom.* **1999**, 104 (1-3), 55-60.

58. Skala, T.; Veltruska, K.; Moroseac, M.; Matolinova, I.; Korotchenkov, G.; Matolin, V., Study of Pd-In interaction during Pd deposition on pyrolytically prepared In<sub>2</sub>O<sub>3</sub>. *Appl. Surf. Sci.* **2003**, 205 (1-4), 196-205.

59. Barr, T. L.; Ying Li, L., An x-ray photoelectron spectroscopy study of the valence band structure of indium oxides. *J. Phys. Chem. Solids* **1989**, 50 (7), 657-664.

60. Brinzari, V.; Korotcenkov, G.; Ivanov, M.; Nehasil, V.; Matolin, V.; Masek, K.; Kamei, M., Valence band and band gap photoemission study of (111) In<sub>2</sub>O<sub>3</sub> epitaxial films under interactions with oxygen, water and carbon monoxide. *Surf. Sci.* **2007**, *601* (23), 5585-5594.
61. Gabasch, H.; Kleimenov, E.; Teschner, D.; Zafeiratos, S.; Hävecker, M.; Knop-Gericke, A.; Schlögl, R.; Zemlyanov, D.; Aszalos-Kiss, B.; Hayek, K.; Klötzer, B., Carbon incorporation during ethene oxidation on Pd(111) studied by in situ X-ray photoelectron spectroscopy at. *J. Catal.* **2006**, *242* (2), 340-348.
62. Ivarsson, D. C. A.; Neumann, M.; Levin, A. A.; Keilhauer, T.; Wochner, P.; Armbrüster, M., In Operando GIXRD and XRR on Polycrystalline In<sub>52</sub>Pd<sub>48</sub>. *Z. Anorg. Allg. Chem.* **2014**, *640* (15), 3065-3069.
63. Smith, J. F.; Schneider, V. L., Anisotropic thermal expansion of indium. *J. Less-Common Met.* **1964**, *7* (1), 17-22.
64. Schroeder, R. H.; Schmitz-Pranghe, N.; Kohlhaas, R., *Z. Metallkd.* **1972**, *63*, 12-16.
65. Marezio, M., Refinement of the crystal structure of In<sub>2</sub>O<sub>3</sub> at two wavelengths. *Acta Crystallogr.* **1966**, *20* (6), 723-728.
66. Harris, I. R.; Norman, M.; Bryant, A. W., A study of some palladium-indium, platinum-indium and platinum-tin alloys. *J. Less-Common Met.* **1968**, *16* (4), 427-440.
67. Häussermann, U.; Elding-Ponten, M.; Svensson, C.; Lidin, S., Compounds with the Ir<sub>3</sub>Ge<sub>7</sub> structure type: Interpenetrating frameworks with flexible bonding properties. *Chem. - Eur. J.* **1998**, *4* (6), 1007-1015.